Role of the plasmasphere in radiation belt particle energization and loss from DMSP, IMAGE, and SAMPEX observations

W. R. Johnston[1], P. C. Anderson[1], J. Goldstein[2], T. P. O'Brien[3], and S. G. Kanekal[4]

[1]W. B. Hanson Center for Space Sciences, University of Texas at Dallas, Richardson, TX [2]Space Science and Engineering Division, Southwest Research Institute, San Antonio, TX
[3]The Aerospace Corporation, Chantilly, VA [4]Laboratory for Atmospheric and Space Physics, University of Colorado at Boulder, Boulder, CO

Abstract

The plasmapause is very dynamic in response to changes in magnetospheric convection and other stormtime phenomena. The outer radiation belt is also dynamic during stormtime in terms of both radial location and energetic particle population. It is proposed that outer radiation belt particles are variously depleted and energized due to wave-particle interactions associated with the plasmapause location. This may be tested by simultaneous observations of energetic particles and the plasmapause location. SAMPEX observations of radiation belt particles may be compared with plasmapause observations from IMAGE, but these provide limited temporal coverage. We use data from DMSP satellites to identify the plasmapause signature in the ionosphere (specifically the light ion trough) to provide more continuous plasmapause observations. This will allow us to build a multiyear database of plasmapause locations. We report on comparisons of these DMSP-derived plasmapause locations to IMAGE-based observations as well as SAMPEX observations of outer radiation belt dynamics and precipitating particle microbursts.

Plasmasphere-radiation belt interactions

The Earth's plasmasphere is dynamically influenced by magnetospheric and ionospheric electric fields. To first order, it comprises the region where closed corotating field lines contain trapped plasma (Fig. 1). Studies have shown that plasmasphere is highly variable both spatially and temporally, responding to changes in geomagnetic indices, ring current, penetration and shielding electric fields, and subauroral electric fields. Consequently the plasmasphere exhibits erosion, emptying, and refilling during active times, along with a high level of structure. The plasmapause, or outer plasmasphere boundary, is typically located at L=4-6 but may be found at L=2 during active times.

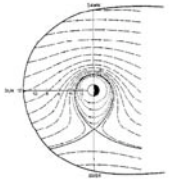

Fig. 1. Convection paths for plasma in magnetosphere, which are along equipotentials of the superposition of the corotation and solar-wind driven electric fields. Within the plasmapause, flux tube motion is dominated by corotation; outside this boundary motion is dominated by convection. Duskside bulge is evident. (From Kavanagh et al., 1968)

The evolution of the plasmapause during active times can significantly affect the outer radiation belt:

- *Summers et al.* (1998) argue that enhanced electromagnetic ion cyclotron (EMIC) waves within the plasmasphere tend to scatter trapped electrons into the loss cone, depleting radiation belt particles inside the plasmapause. At the same time, outside the plasmapause whistler-mode waves tend to energize trapped electrons (Fig. 2).
- *Goldstein et al.* (2005) found that the outer radiation belt responded to radial movement of the plasmapause during disturbed times with a time lag of several days.

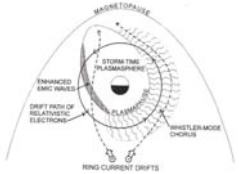

Fig. 2. Schematic of proposed mechanism for outer radiation belt energization and loss associated with the plasmasphere. (From *Summers et al.,* 1998.)

Plasmapause-ionosphere interactions

Several ionospheric signatures of the plasmapause have been proposed, including:

- midlatitude electron density trough
- total electron content (TEC)
- subauroral electron temp. enhancement (SETE)
- precipitating electron boundary
- stable auroral red arcs (SARS)
- light ion trough (LIT)

There is generally not a one-to-one correspondence between any of these and the plasmapause. *Taylor and Walsh* (1972) found LIT one of the more consistent signatures, whereas *Foster et al.* (1978) found the LIT generally a few degrees equatorward of the plasmapause as identified by whistler waves. Grebowsky et al. (1978) suggested supersonic upward H+ flows result in LIT-plasmapause mismatch during refilling.

Satellites/instrumentation: DMSP, IMAGE, SAMPEX

DMSP: polar sun-synchronous orbits, alt. 840 km, period 100 min., generally 3-4 operational at any given time. During 2001 data is available from F12, F14, and F15 in pre-midnight to morning and F13 in dusk to dawn. Instruments include:

- Retarding Potential Analyzer (RPA) providing ion density and composition
- Ion Drift Meter (IDM)
- Precipitating Electron and Ion Detectors (SSJ/4)

IMAGE: eccentric polar orbit (from 1400 km alt. to 8 R_E), operational 3/2000 to 12/2005. Instruments include:

- EUV imagers directly imaging 30.4 nm UV scattered by plasmaspheric He^+. Such imaging is feasible when IMAGE is near apogee (Fig. 3).

Fig. 3. Sample IMAGE EUV image of plasmasphere, showing extracted plasmapause locations. (From *Goldstein et al.,* 2004)

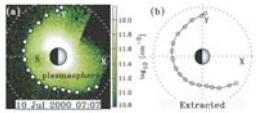

SAMPEX: low Earth orbit, alt. from 500 km to 620 km in 2001, operational 7/1992, includes four instruments for energetic particle measurements:

- Heavy Ion Large Area Proportional Counter Telescope (HILT)
- Low Energy Ion Composition Analyzer (LEICA)
- Mass Spectrometer Telescope (MAST)
- Proton/Electron Telescope (PET)

Methodology: DMSP-derived plasmapause locations

Choosing the LIT to identify the plasmapause, we used DMSP data to identify the high-latitude gradient in H^+ density. Our semi-automatic algorithm identifies the plasmapause as a point where the smoothed H+ density on the equatorward side of the LIT is 50% greater than the LIT density minimum.

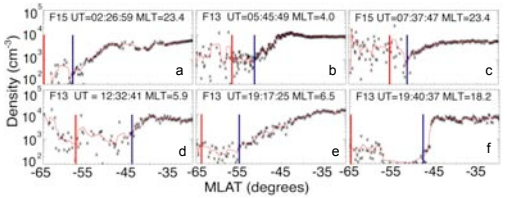

Fig. 4 shows sample DMSP observations of H^+ density. Each plot shows:

- H+ density observations (points) with 5-point smooth (red line)
- electron precipitation boundary *(vertical red line)*
- derived plasmapause locations *(blue vertical line)*

The sequence 4a-4f shows plasmasphere evolution through a storm:

a) stagnation boundary slightly poleward of plasmapause boundary: plasmasphere still refilling after previous depletion;

b,c) stagnation boundary has moved due to stormtime penetration E fields, subauroral E fields nearly to plasmapause boundary;

f) during storm recovery E field and stagnation boundary return to high latitudes, leaving eroded plasmasphere with sharp boundary to begin refilling.

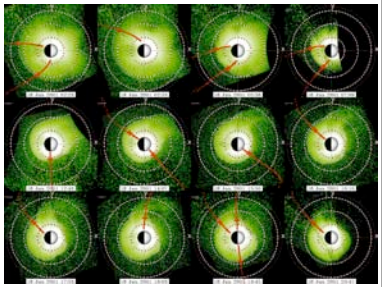

Fig. 5 shows IMAGE EUV observations of He^+ plasmapause on 18 June 2001 projected to SM X-Y plane (see *Goldstein and Sandel*, 2005). Sun is to right, dusk at top. Red traces show DMSP F13 and F15 orbit tracks mapped to X-Y plane in SM coordinates using the IGRF 2000 and Tsyganenko 2001 magnetic field models. Red crosses indicate location of ionospheric projection of plasmapause derived from the DMSP H^+ observations, using the equatorward minimum in the light ion density as described in the previous figure. Plot shows all F13/F15 identifications within 30 min. of an IMAGE observation.

Case study: comparison with IMAGE, SAMPEX

Dynamic behavior of the plasmapause and radiation belt in early 2001 was studied by *Goldstein et al.* (2005). We have applied our DMSP-based approach to this 72-day period (using the LIT density minimum method) permitting comparison of DMSP- and IMAGE-derived plasmapause locations.

Fig. 6 shows these results superimposed on IMAGE/SAMPEX data (from *Goldstein et al.,* 2005):

- Top frame shows IMAGE-derived plasmapause locations from each EUV image *(red, average L; blue, minimum L)* and all 1790 DMSP-derived plasmapause locations *(black)*, which complement gaps in IMAGE coverage.
- Second frame shows SAMPEX electron counts (2-6 MeV) as daily averages, with the daily average DMSP-derived plasmapause location shown *(white line)*. The inner edge of the outer radiation belt moves inward a few days after inward motion of plasmapause during disturbances 1 and 2--but not following inward motion of plasmapause during disturbance 4.
- Third frame shows Dst index. Note correlation between DMSP-derived plasmapause locations and Dst, including several intermediate disturbances.

Fig. 7 compares DMSP-derived plasmapause locations *(black)* to the L values of relativistic electron microbursts *(red)* identified by SAMPEX (see *O'Brien et al.,* 2003). These microbursts (~1 sec duration) represent transient scattering events. Microburst locations correlate with plasmapause locations, both rapidly moving inward with storm events and slowly moving outward during recovery; consistent with burst production by whistler chorus wave-particle interactions outside the plasmasphere.

Fig. 6

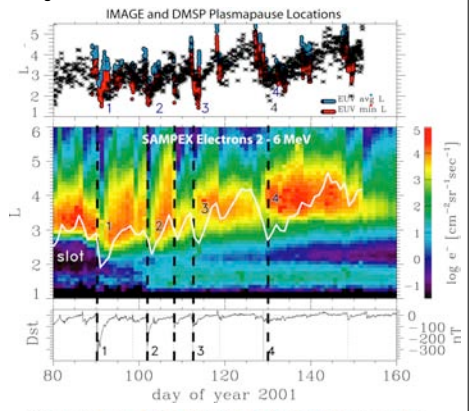

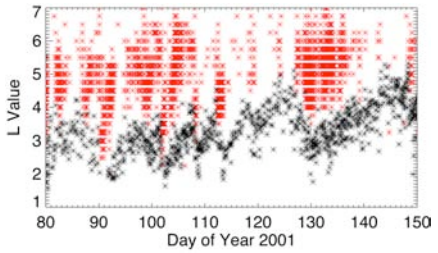

Fig. 7

Conclusions and future work

Initial results from the case studies for early 2001 show

- Compared to the IMAGE-identified plasmapause, the DMSP-identified plasmapause based on the LIT minimum is very similar to locations identified by IMAGE. Average difference is ~0.5 L.
- Outer radiation belt location found by SAMPEX generally responds to changes in plasmapause location with a delay of two or three days--this holds for most disturbances, but not for all (e.g. disturbance 4).
- Plasmapause locations correlate with SAMPEX-identified microburst locations. Microburst locations are nearly always located outward of plasmapause locations. Both move inward rapidly during storm events, with microbursts filling gaps in plasmapause locations at high L values, then slowly move outward in concert during recovery.
- DMSP-identified plasmapause dynamics correlates well with Dst for disturbances of varying intensities.

In the investigation for 18 June 2001, we find good agreement between plasmapause identifications from DMSP and IMAGE, with the LIT density minimum identifications. We will refining the algorithm and developing a multiyear database of plasmapause locations.

The extent of DMSP time coverage will permit comparisons to SAMPEX, including the period from 1996 to 1998 when SAMPEX spacecraft rotation permitted derivation of pitch angle information. These data will be used to examine the relationship of the plasmasphere and radiation belt energization and loss.

References

- Foster, J. C., et al. (1978), *JGR* 83:1175-1182.
- Goldstein, J., et al. (2004), *GRL* 31:L01801.
- Goldstein, J., S. G. Kanekal, D. N. Baker, B. R. Sandel (2005), *GRL* 32:L15104.
- Goldstein, J., and B. R. Sandel (2005), in *Inner Magnetosphere Interactions*, doi:10.1029/2004BK000104.
- Grebowksy, J. M., et al. (1978), Planet. Space Sci., 26:651-660.
- Kavanagh, L. D., Jr., et al. (1968), *JGR* 73:5511-5519.
- O'Brien, T. P., et al. (2003) *JGR* 108(A8):1329-1342.
- Summers, D., R. M. Thorne, F. Xiao (1998), *JGR* 103(A9):20487-20500.
- Taylor, H. A., Jr., and W. J. Walsh (1972), *JGR* 77:6716-6723.